

PAPER

ANTHROPOLOGY

Rafael Fernández Castillo,¹ Ph.D.; Douglas H. Ubelaker,² Ph.D.; José Antonio Lorente Acosta,³ M.D.; Rafael José Esteban de la Rosa,⁴ M.D.; and Inmaculada Garcia Garcia,⁵ Ph.D.

Effect of Temperature on Bone Tissue: Histological Changes

ABSTRACT: The analysis of burned human remains has been of great interest among forensic anthropologists largely due to the difficulty that their recovery, classification, reconstruction, and identification present. The main purpose of this analysis is to present histological methodology for the interpretation of bones altered by thermal processes. We include analyses of the microscopic changes among bones exposed to different temperatures, with the goal of establishing categories of histological morphology in relation to fire temperature. Samples of bone (ilium) were exposed systematically to controlled temperatures. Analysis of the resulting histological changes has allowed the formation of a clear four-stage classification of the alterations observed. This classification should prove useful in assessing bone changes in relation to temperature of exposure, particularly in cases where this temperature was previously not known.

KEYWORDS: forensic science, forensic anthropology, burned bones, cremains, thermal, histology

The analysis of burned human remains has been of great interest among forensic anthropologists largely due to the difficulty that their recovery, classification, reconstruction, and identification present. Previous investigations have focused on the study of bone surface color and the macroscopic and microscopic morphology of the crystalline structure in a controlled environment (1–5). However, a review of the anthropological literature reveals that the current methodologies for analysis of burned human bone are still, at best, confusing (1–8). Presently there are few publications centered on the histological structural changes caused by fire.

Macroscopically, during the cremation process, the fire and heat modify and destroy the bone structure in size, color, and shape (9,10). Between 100°C and 300°C, the bone becomes dehydrated, leading to a reduction of the bone to 1–2% of its volume (11). Then follows a phase of 300–600°C, where an alteration of the main structural features of mineralized bone tissue occurs (12). At a temperature of 600–800°C, the organic material fully burns and bone structure contraction increases (13). At temperatures higher than 800°C, the crystals transform into larger crystals and the bone structure becomes more fragile (14). The melting point is *c.* at 1630°C (15).

These changes have been defined by a wide variety of somewhat contradictory studies (1–15). Some histological changes have been examined, but generally using equipment and instruments that are not broadly available (1,9–11). Our research proposes an easily applied method using a simple microscope that can examine the changes produced in cortical and trabecular bone as a consequence of the increase in temperature. The study of these changes is necessary due to the important effects that fire and heat produce in the alteration of material evidence and human remains.

Methods

A total of 165 samples were obtained from forensic cadaver autopsies, with an age range of 26–88 years. All individuals had died from unexpected (not necessarily sudden) or violent death. Of the collected samples, 15 were discarded for one or more of the following reasons: time of death exceeded more than 24 h; insufficient quantity of collected samples; error in sample processing; and evidence of disease that could affect bone metabolism. Of the 150 studied samples, 87 were those of male cadavers and 63 were those of female cadavers.

The samples were obtained by bone biopsy with the use of Bordier's trocar in the left ilium (Fig. 1), no more than 24 h postmortem. In this step, a transiliac cylinder of 7 mm in diameter and 15 mm in length was obtained, *c.* 2 cm from the iliac border (Fig. 1). The samples were burned in a furnace at controlled temperatures ranging from 100° to 1100° C for 20 min each. The following lists the number of samples exposed to each temperature: 13 at 100°C, 10 at 200°C, 13 at 300°C, 15 at 400°C, 13 at 500°C, 15 at 600°C, 13 at 700°C, 15 at 800°C, 15 at 900°C, 15 at 1000°C, and 13 at 1100°C.

The bone samples were processed without decalcification using dehydration in 96% alcohol and inclusion within methyl

¹Laboratory of Anthropology, Faculty of Medicine, University of Granada, Av de Madrid, 11, Granada 18012, Spain.

²Department of Anthropology, Smithsonian Institution, NMNH, MRC 112, Washington, DC 20560-0112.

³Legal Medicine Department, Faculty of Medicine, University of Granada, Av de Madrid, 11, Granada 18012, Spain.

⁴Academic Medical Center Virgen de las Nieves, Avenida de las Fuerzas Armadas 2, Granada 18014, Spain.

⁵School of Health Sciences, University of Granada, Av de Madrid, 11, Granada 18012, Spain.

Received 17 May 2011; and in revised form 10 Jan. 2012; accepted 10 Mar. 2012.

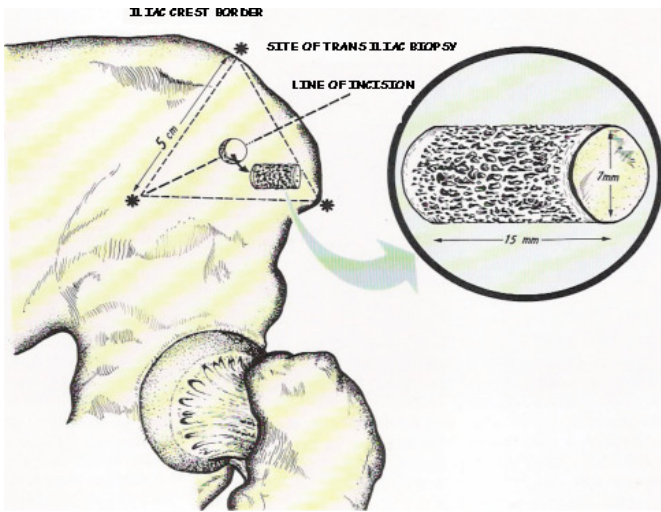


FIG. 1—Location of bone biopsy taken from the ilium.

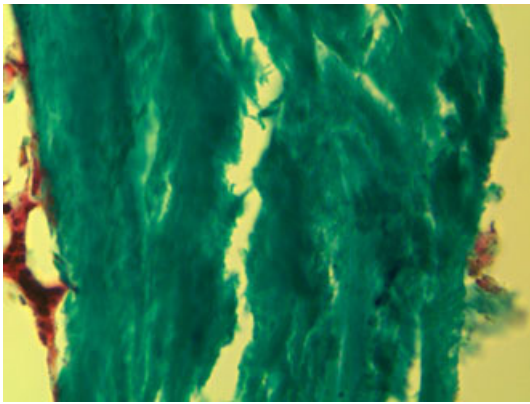


FIG. 2—Longitudinal fractures in trabecular bone at 100°C. Goldner's trichrome 63x.

methacrylate. Sections 3 mm thick were prepared using a Reichert microtome. The sections were fixed on microscope slides and stained using hematoxylin-eosin, Goldner's trichrome, and toluidine blue methods.

The samples were analyzed using a Leica DMLB microscope, and the images were captured with a CCD Sony camera, adapted for use with a digitalizing card. Once the bone section images were obtained and digitalized at 10x, 20x, 40x, 63x and 100x, they were analyzed.

Results

At 100°C, osseous cells are visible, as well as the remains of muscular tissue and blood cells. Longitudinal microfractures appear in the trabecular (Fig. 2) and cortical bone (Fig. 3). Haversian channels appear deformed (Fig. 3).

At 200°C, the remains of muscular tissue are still visible, as well as osteoid elements. Osseous cells are still present. Longitudinal microfractures appear in clustered form (Fig. 4). Polyhedral crystalline formations begin to appear (Fig. 5).

At 300°C, agglutinated soft tissue remains. The trabecular bone structure begins to deform, producing polyhedral crystalline formations in the matrix of the connective tissue (Figs 6 and 7). Osteoid formations still remain (Fig. 7).

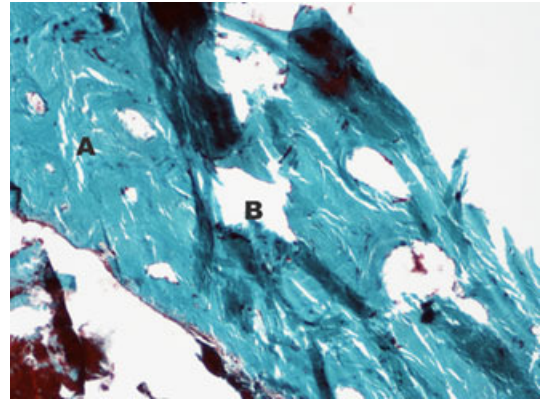


FIG. 3—(A) Longitudinal fractures in cortical bone. (B) Haversian systems appear deformed. 100°C. Goldner's trichrome 20x.

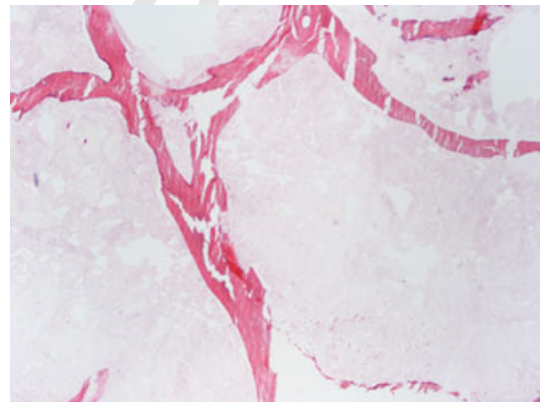


FIG. 4—Detail of a trabecular fracture at 200°C. Hematoxylin-eosin 4x.

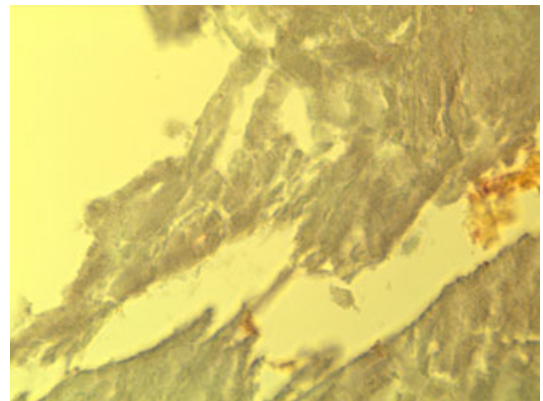


FIG. 5—Crystalline formations in cortical bone at 200°C. Hematoxylin-eosin 63x.

At 400°C, agglutination of longitudinal radial fractures occurs with square-shaped crystalline formations (Fig. 8).

At 500°C, mineralized rings in the bone are clearly seen. Cubic and clustered form structures are visible. (Figs 9 and 10).

At 600°C, the cortical bone has cubic crystalline formations. The trabecular bone begins to appear increasingly rough (Fig. 11).

At 700°C, there is a proliferation of the formation and size of the cubic crystalline structures. Both areas of bone show increasingly more agglutination (Fig. 12).

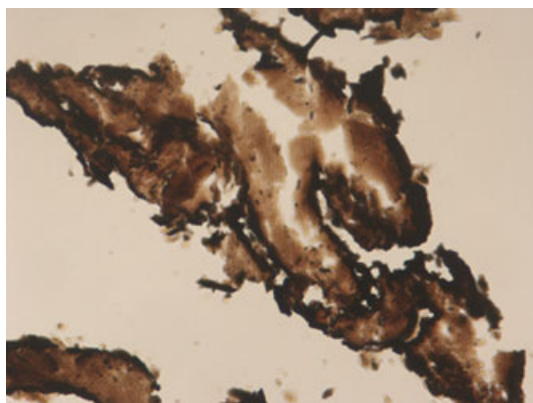


FIG. 6—Deformed trabecular structure. 300°C. Hematoxylin-eosin 40×.



FIG. 9—Linear macromolecular crystalline polymers of collagen and extracellular matrix. 500°C. Toluidine blue 20×.

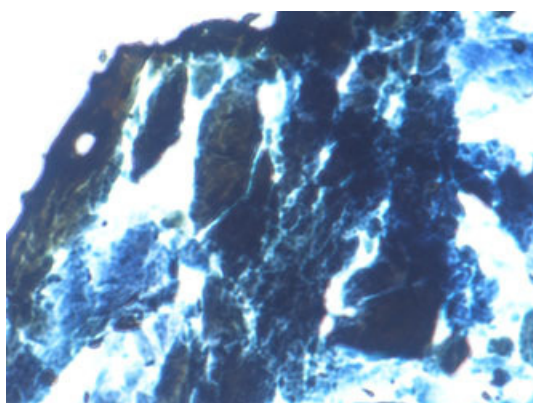


FIG. 7—Crystalline formations in cortical bone. 300°C. Toluidine blue 40×.

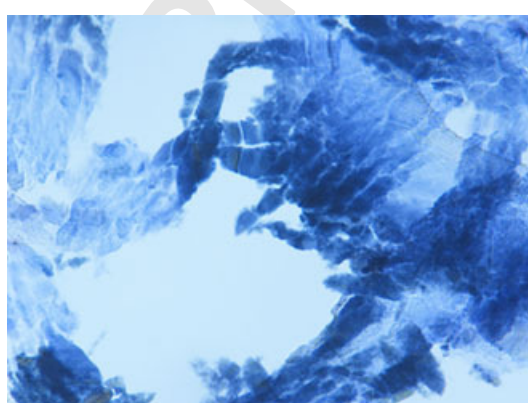


FIG. 10—Linear macromolecular crystalline polymers of collagen and extracellular matrix. 500°C. Toluidine blue 40×.

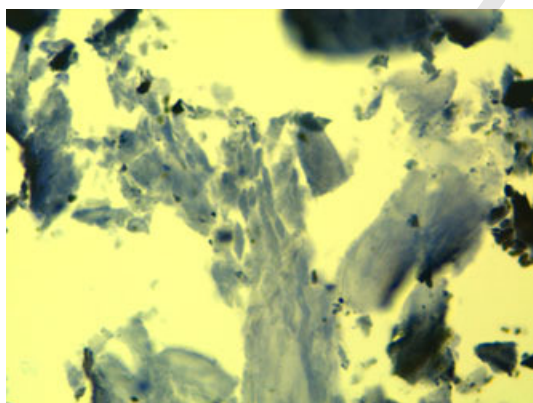


FIG. 8—Crystalline formations in the trabecular bone. 400°C. Toluidine blue 63×.

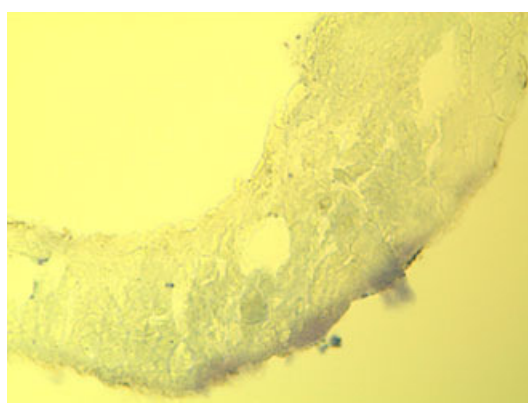


FIG. 11—Crystalline formations in the trabecular bone. 600°C. Hematoxylin-eosin 40×.

At 800°C, the structure continues to become more agglutinated and chaotic. The cortical bone areas appear fused to the areas of spongy bone. There is significant shrinkage in granular form of the spongy bone. The crystalline structures reach their maximum size (Fig. 13).

At 900°C, there is an abundance of granulation of the trabecular bone. Crystalline structures no longer appear (Fig. 14).

At 1000°C, there is an absence of polyhedral crystals and crystalline areas. The tissue is increasingly more granular (Figs 15 and 16).

At 1100°C, the cortical and trabecular bone appear as granular tissue (Figs 17 and 18).

Discussion

In this study, the ilium was chosen to represent the changes that occur in both the cortical and spongy bone of most of the skeleton (16,17). During the burning process, fire affects all the muscles in an exposed body, causing muscle fibers to warm and

1
2
3
4
5
6
7
8
9
10
11
12
13
14
15
16
17
18
19
20
21
22
23
24
25
26
27
28
29
30
31
32
33
34
35
36
37
38
39
40
41
42
43
44
45
46
47
48
49
50
51
52
53
54
55
56
57
58
59
60
61
62
63

Colour online, B&W in print
Colour online, B&W in print
Colour online, B&W in print
Colour online, B&W in print
Colour online, B&W in print

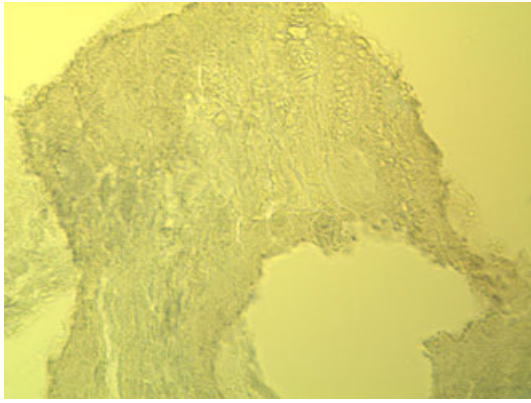


FIG. 12—Crystalline formations in cortical bone. 700°C. Hematoxylin-eosin 40×.

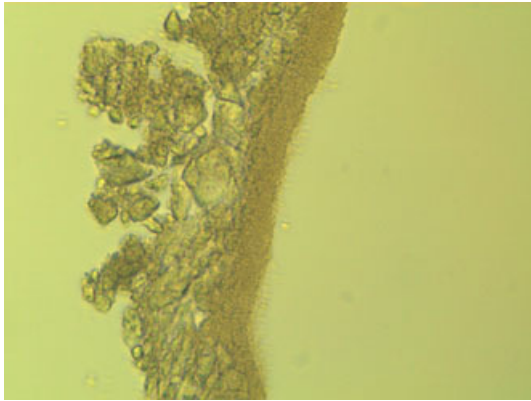


FIG. 13—Crystals in trabecular bone. 800°C. Hematoxylin-eosin 63×.

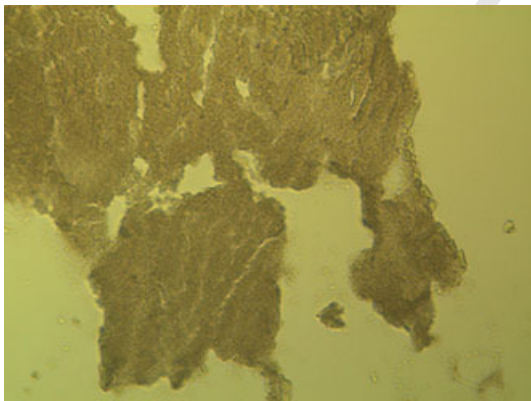


FIG. 14—Granulation in trabecular bone. 900°C. Hematoxylin-eosin 40×.

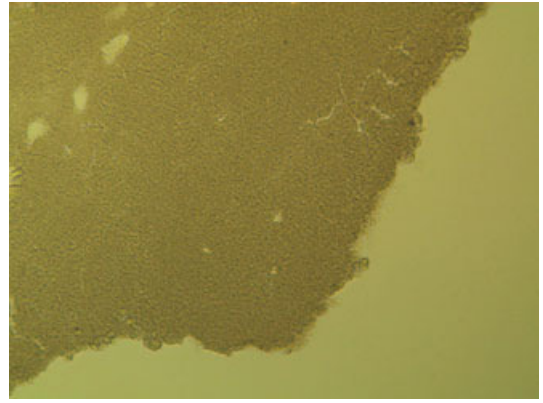


FIG. 15—Increased granularity in trabecular bone. 1000°C. Hematoxylin-eosin 40×.

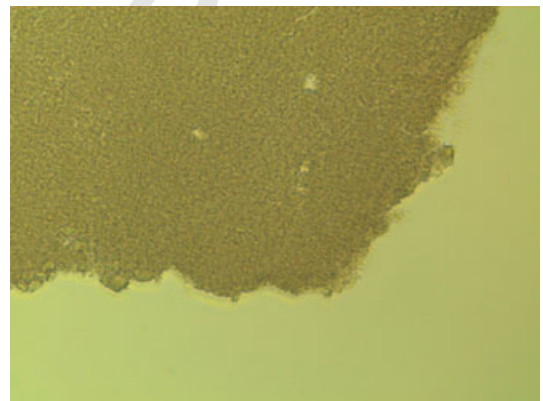


FIG. 16—Increased granularity in cortical bone. 1000°C. Hematoxylin-eosin 63×.

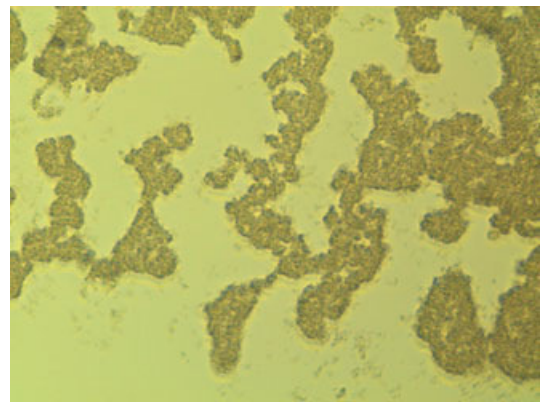


FIG. 17—Trabecular deformations. 1100°C. Hematoxylin-eosin 63×.

reduce. The final position of remains is thus affected by muscle and ligament contraction that initiates after *c.* 10 min at a temperature of 800°C. This muscle contraction will result in greater exposure of certain anatomical areas and protection of others, not only in relation to the tissue depth but also in relation to how those areas are positioned. These areas of exposure can, in turn, help in obtaining a representative sample to understand varying temperatures reached by the fire (18,19). The ilium was chosen for this study because it presents both cortical and

trabecular bone in an anatomical area not associated with limb attachment and variable heat exposure.

When the bone is exposed to temperatures of 100–200°C, the fundamental characteristic is the presence of longitudinal fractures both in the cortical and trabecular bone (Figs 2–4), while crystalline formations appear from 200°C upward (Fig. 5).

From 300°C to 400°C, the organic materials disappear (20,21), fractures become more obvious and the connective bone tissues tend to become deformed (Fig. 6). Likewise, crystalline formations increase in size at this temperature (22, Figs 7 and 8).

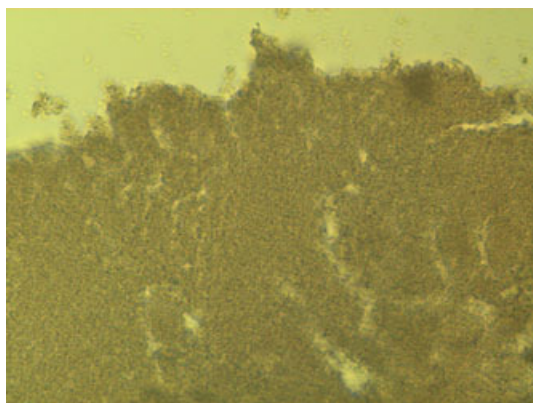


FIG. 18—Granular appearance in cortical bone. 1100°C. Hematoxylin-eosin 63×.

TABLE 1—Sequential thermal-related histological changes.

Temperatures	Histological Changes
From 100°C to 300°C	Longitudinal fractures, presence of osseous cells and organic tissue. First polyhydric crystalline formations
From 400°C to 600°C	Presence of cubic crystalline formations. Crystalline polymers
From 700°C to 800°C	The bone structure has become crystalline and loses homogeneity
Greater than 900°C	Clustered formation with loss of osseous structure

From 500°C to 600°C, the crystalline linear macromolecular polymers form in the collagen and extracellular matrix (Figs 9 and 10), which show metachromatic changes that suggest the existence of sulfo and/or carboxymucins. The heat transforms these crystals in the liquid or isotropic crystal phases (22).

Between 600°C and 800°C (Figs 11–13), crystalline formations increase in size and number. Likewise, the appearance of the bone also changes from a laminar pattern with a homogeneous texture to a more crystalline texture, as other investigators have also reported (23–25).

At temperatures approaching 900°C, large crystal structures are no longer identifiable. As temperatures reach 900°C and higher, the structure becomes completely crystalline, yet amorphous and granular in shape. This can be explained by the recrystallization phenomena of the compounds derived from the hydroxyapatite thermal hydrolysis, which results in retraction, fracture, bone matrix vesicle formation, Haversian canals bursting and, finally, cluster formations (26,27).

To conclude, we have focused on the histological changes in the cortical and trabecular bones and the formations of crystalline structures at different temperatures. These temperature-related changes can be classified into four distinct stages (Table 1). This classification can be made by a simple bone biopsy and it offers information about the temperatures to which human remains were exposed. Of course, in casework other factors also should be considered, such as duration of elevated temperatures and context.

References

1. Van Vark GN. The investigation of human cremated skeletal material by multivariate statistical methods. *J Methodology. Ossa* 1974;1:63–95.
2. Herrmann B. On histological investigations of cremated human remains. *J Hum Evol* 1977;6:101–3.

3. Holland TD. Use of the cranial base in the identification of fire victims. *J Forensic Sci* 1989;2:458–60.
4. Bohnert M, Rost T, Pollak S. The degree of destruction of human bodies in relation to the duration of fire. *Forensic Sci Int* 1998;95:11–21.
5. Correia PM, Beattie O. A critical look at methods for recovering, evaluating, and interpreting cremated human remains. In: Haglund WD, Sorg MH, editors. *Advances in forensic taphonomy: method theory, and archaeological perspectives*. Boca Raton, FL: CRC Press, 2002;435–50.
6. Ubelaker DH. The forensic evaluation of burned skeletal remains: a synthesis. *Forensic Sci Int* 2009;183:1–5.
7. Fairgrieve SI. *Forensic cremation: recovery and analysis*. Boca Raton, FL: CRC Press, 2008.
8. Schmidt CW, Symes SA, editors. *The analysis of burned human remains*. London, U.K.: Academic Press, 2008.
9. Hiller JC, Thompson TJU, Evison MP, Chamberlain AT, Wess TJ. Bone mineral change during experimental heating: an X-ray scattering investigation. *Biomaterials* 2003;24:5091–7.
10. Thompson TJU. Heat-induced dimensional changes in bone and their consequences for forensic anthropology. *J Forensic Sci* 2005;5:1008–15.
11. Piga G, Malgosa A, Thompson TJU, Enzo S. A new calibration of XRD technique for the study of archaeological burned human remains. *J Archaeol Sci* 2008;35:2171–8.
12. Christensen AM. Experiments in the combustibility of the human body. *J Forensic Sci* 2002;3:466–70.
13. Shipman P, Foster G, Schoeninger M. Burnt bones and teeth: an experimental study of color, morphology, crystal structure and shrinkage. *J Archaeol Sci* 1984;11:307–25.
14. Van Vark GN, Pasveer JM, Arend A, Amesz-Voorhoeve WHM, Kuizenga D, Dokládál M. Sex diagnosis of the human sternum. *Riv di Antrop* 1995;73:65–73.
15. Correia PM. Fire modification of bone: a review of the literature. In: Haglund WD, Sorg MH, editors. *Forensic taphonomy: the postmortem fate of human remains*. Boca Raton, FL: CRC, 1997;275–93.
16. Thomsen JS, Ebbesen EN, Mosekilde L. Static histomorphometry of human iliac crest and vertebral trabecular bone: a comparative study. *Bone* 2002;30:267–74.
17. Bordier PJ, Tun CS. Quantitative histology of metabolic bone disease. *Clin Endocrinol Metab* 1972;1:197–215.
18. Leffler SG, Chew FS. CT-guided percutaneous biopsy of sclerotic bone lesions: diagnostic yield and accuracy. *Am J Roentgenol* 1999;172:1389–92.
19. Vedi S, Compston JE, Webb A, Tighe JR. Histomorphometric analysis of dynamic parameters of trabecular bone formation in the iliac crest of normal British subjects. *Metab Bone Dis Relat Res* 1983;5:69–74.
20. Holden JL, Phakey PP, Clement JG. Scanning electron microscope observations of heat-treated human bone. *Forensic Sci Int* 1995;74:29–45.
21. Grevin G, Bailet P, Quatrehomme G, Ollier A. Anatomical reconstruction of fragments of burned human bones: a necessary means for forensic identification. *Forensic Sci Int* 1998;96:129–34.
22. Warren MW, Schultz JJ. Post-cremation taphonomy and artifact preservation. *J Forensic Sci* 2002;3:656–9.
23. Stiner MC, Kuhn SL, Weiner S, Bar-Yosef O. Differential burning, recrystallization and fragmentation of archaeological bone. *J Archaeol Sci* 1995;22:223–37.
24. Fratzi P, Schreiber S, Klaushofer K. Bone mineralization as studied by small-angle X-ray scattering. *Connect Tissue Res* 1996;34(4):247–54.
25. Holden JL, Phakey PP, Clement JG. Scanning electron microscope observations of incinerated human femoral bone: a case study. *Forensic Sci Int* 1995;74:17–28.
26. Kalsbeek N, Richter J. Preservation of burned bones: an investigation of the effects of temperature and pH on hardness. *Stud Conserv* 2006;5:123–37.
27. McKinley JI. Bone fragment size and weights of bone from modern British cremations and the implication for the interpretation of archaeological cremations. *Int J Osteoarch* 1993;3:283–7.

Additional information and reprint requests:

Rafael Fernández Castillo, Ph.D.

Faculty of Medicine

Anthropology Department

University of Granada

Avda. de Madrid

s/n – 18071 Granada

Spain

E-mail: rafaelfernandez@ugr.es

Author Query Form

Journal: JFO

Article: 12093

Dear Author,

During the copy-editing of your paper, the following queries arose. Please respond to these by marking up your proofs with the necessary changes/additions. Please write your answers on the query sheet if there is insufficient space on the page proofs. Please write clearly and follow the conventions shown on the attached corrections sheet. If returning the proof by fax do not write too close to the paper's edge. Please remember that illegible mark-ups may delay publication.

Many thanks for your assistance.

Query reference	Query	Remarks
1	AUTHOR: References [2] and [22] are identical. Hence, reference [22] is deleted and rest of the references is renumbered. Please check.	
2	AUTHOR: Figure 1 has been saved at a low resolution of 140 dpi. Please resupply at 600 dpi. Check required artwork specifications at http://author-services.wiley.com/submit_illust.asp?site=1	

Proof Correction Marks

Please correct and return your proofs using the proof correction marks below. For a more detailed look at using these marks please reference the most recent edition of The Chicago Manual of Style and visit them on the Web at: <http://www.chicagomanualofstyle.org/home.html>

<i>Instruction to typesetter</i>	<i>Textual mark</i>	<i>Marginal mark</i>
Leave unchanged	... under matter to remain	<u>stet</u>
Insert in text the matter indicated in the margin	^	^ followed by new matter
Delete	Ʒ through single character, rule or underline or Ʒ through all characters to be deleted	Ʒ
Substitute character or substitute part of one or more word(s)	Ƶ through letter or — through characters	new character Ƶ or new characters Ƶ
Change to italics	— under matter to be changed	<u>ital</u>
Change to capitals	≡ under matter to be changed	<u>Caps</u>
Change to small capitals	≡ under matter to be changed	<u>sc</u>
Change to bold type	~ under matter to be changed	<u>bf</u>
Change to bold italic	~ under matter to be changed	<u>bf+ital</u>
Change to lower case	Ɔ	<u>lc</u>
Insert superscript	∨	∨ under character e.g. ∨
Insert subscript	^	^ over character e.g. ^
Insert full stop	⊙	⊙
Insert comma	↵	↵
Insert single quotation marks	↙ ↘	↙ ↘
Insert double quotation marks	↵ ↶	↵ ↶
Insert hyphen	=	=
Start new paragraph	¶	¶
Transpose	┌┐	┌┐
Close up	linking ○ characters	○
Insert or substitute space between characters or words	#	#
Reduce space between characters or words	◌	◌